Optimization of a solar chimney design to enhance natural ventilation in a multi-storey office building

M. Gontikaki BSc. dr. Dipl.-Ing. M. Trcka prof.dr.ir. J.L.M. Hensen Ir. Pieter-Jan Hoes

Unit Building Physics and Systems
Eindhoven University of Technology
Eindhoven, Netherlands

ABSTRACT
Natural ventilation of buildings can be achieved with solar-driven, buoyancy-induced airflow through a solar chimney channel. Research on solar chimneys has covered a wide range of topics, yet study of the integration in multi-storey buildings has been performed in few numerical studies, where steady-state conditions were assumed. In practice, if the solar chimney is to be used in an actual building, dynamic performance simulations would be required for the specific building design and climate. This study explores the applicability of a solar chimney in a prototype multi-storey office building in the Netherlands. Sensitivity analysis and optimization of the design will be performed via dynamic performance simulations in ESP-r. The robustness of the optimized design will be tested at the final stage, against e.g. windows' opening by users. This is an ongoing project; calibration of the solar chimney model and preliminary sensitivity analysis results are presented here.

INTRODUCTION

The exploitation of sustainable energy sources to cover the functional demands of buildings (for heating, ventilation, cooling etc) can contribute to significant energy savings and thus to alleviation of the current environmental, economical and social problems related to conventional energy practices. Passive (natural) ventilation of buildings is a successful means to save energy otherwise consumed for mechanical ventilation and/or cooling. Solar chimneys (SC) are passive elements that make use of the solar energy to induce buoyancy-driven airflow and naturally ventilate the building.

A SC differs to a conventional chimney in that at least one wall is made transparent; solar radiation enters the chimney through the glazed part and heats up the walls. The temperature of the air inside the SC channel rises due to heat transfer from the walls and the resulting buoyancy drives the airflow through the channel. The SC pulls air from the interior of the building, which is replaced by fresh air through openings or other paths, and natural ventilation is accomplished. Performance of the SC is primarily described by the induced ventilation flow rates; in case heat harvesting is also of interest, air temperature in the channel is the other important performance indicator.

The geometry of the SC channel is described by its height, length and cavity width. The elements of the SC are presented in Fig. 1; the terms indicated in Fig. 1 will be used in the following sections to refer to the solar chimney's parts and geometrical features. Integration of a solar chimney in a building is possible in many ways (Fig. 2), e.g. as part of the south-facing façade (or the façade where maximum solar availability applies), on the roof (also known as 'roof solar chimney'), in the place of a conventional chimney or as extension of a double façade (usually for multi-storey buildings).

The present study explores the passive ventilation potential of a SC integrated in a multi-storey office building in the Netherlands. It forms part of a broader project under the name 'Earth, Wind & Fire', concerning the exploitation of solar, geothermal and wind energy in a prototype building. This is an ongoing research and results are not yet available. The following sections present an extensive literature review, the applied methodology and envisaged results.

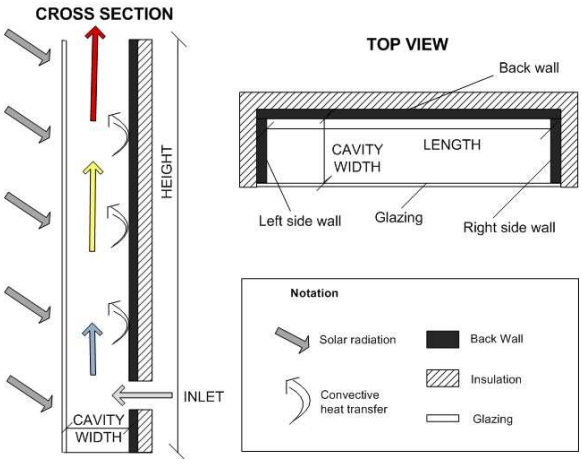

Figure 1. Cross-section and top view of a SC.

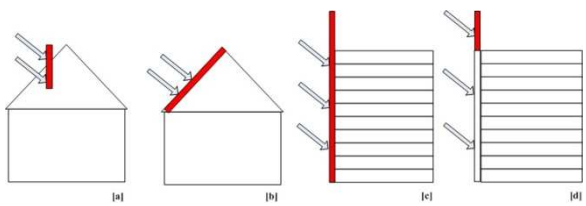

Figure 2. Integration possibilities of SC in buildings.

LITERATURE REVIEW

General Literature Review

During the past few decades numerous research studies have been performed on the SC concept, that have deepened our knowledge on the performance, the parameters that affect the performance and the applicability of the system for natural ventilation and passive cooling of spaces. The studies can fall under the broad categories of experimental, analytical and numerical modeling studies. A general overview of previous studies based on the above categorization will be presented initially. This section offers a general impression of the various research topics and approaches, and no findings will be reported for brevity reasons. Instead, the findings of parametric analysis studies and of the ones regarding integration in multi-storey buildings will be grouped and presented in two consecutive separate sections, since they are greatly related to the present study.

Experimental studies.

Field studies concerning the ventilation induced by SC configurations in a small-scale single-room house were performed in Thailand (Khedari et al., 2000). In a consecutive study Khedari et al. (2003) studied the performance of SC systems in an air-conditioned small-scale house. Barozzi et al. (1992) tested a 1:12 small-scale model of a building where the roof functions as a solar chimney. Hirunlabh et al. (1999) performed a similar study for a 31m^3 volume house where a metallic solar wall was placed on the southern façade. Laboratory experiments on small-scale models were also performed, where temperature distribution of the air and the walls' surfaces, the velocity profile in the chimney's channel and the magnitude of the air flow rates were studied, in combination with parametric analysis (Chen et al. 2003, Burek and Habeb 2007). The performance of a full-scale 2m high SC that was part of a 12m^3 room, was studied under laboratory conditions by Bouchair (1994), while Arce et al. (2009) studied a 4.5m high model, under real meteorological conditions in Spain.

Analytical studies.

In a number of analytical studies mathematical models were developed for the prediction of the solar chimneys' performance. Experiments were usually performed, in order to validate the models. Bansal et al. (1993) developed a steady-state mathematical model to calculate the mean air flow rates and temperatures of a solar chimney connected to a conventional one. Wall temperature was assumed uniform. Awbi and Gan (1992) analytically derived the air temperature distribution along the SC channel by making the same assumption. A steady-state mathematical model was also developed by Bassiouny and Koura (2008) to predict the air changes per hour[1] (ACH) induced in a room by a SC. The thermal resistance network approach was adopted to set up the steady-state heat transfer equations in the model of Ong and Chow (2003), which predicts the performance of a solar chimney under varying ambient conditions. Mathur et al. (2006) followed a similar approach to calculate the ACH induced in a room by a small-sized solar chimney integrated to a normal window. A simplified thermal model and a computer program to calculate ventilation flow rate through a chimney were developed by Afonso and Oliveira (2000) which also takes into account varying climatic conditions, the thermal inertia of the back wall and dependence of the convective heat transfer coefficient on the air flow rate.

Numerical modeling studies.

The buoyancy-driven airflow and heat transfer in vertical heated cavities were investigated numerically, mainly through Computational Fluid Dynamics (CFD) simulations in an increasing number of studies during the past decade. Some of the studies focused on the airflow regime and the heat transfer mechanisms in the SC channel, while others on parametric investigations. The latter will be mentioned here briefly, since more details will be given in the following section. Numerical investigations on the airflow within the Trombe wall channel, which can be considered a type of SC, preceded by many years, with the first one being that of Borgers and Akbari (1979). Rodrigues et al. (2000) studied the airflow regime and the transition from laminar to turbulent flow in a SC channel using a finite-volume method. The heat transfer mechanisms (by conduction, convection and radiation) in the SC channel were studied in detail, using the numerical method of finite-difference control volumes, by Nouanégué and Bilgen (2009).

In certain studies numerical modeling was employed to perform parametric analysis on the SC system. The effects of solar heat gain and glazing type (Gan and Riffat, 1998), cavity width (Gan, 2006), inclination and low emissivity coating (Harris and Helwig, 2007) were some of the issues investigated using CFD modeling. Recently Gan (2010) found that the size of the computational domain (for CFD simulations) has an impact on the airflow and heat transfer coefficient predictions in solar heated cavities, and made corresponding suggestions. An extensive parametric analysis for a SC integrated in a prototype residential building was performed by Ho Lee and Strand (2009), using numerical modeling in the program EnergyPlus. The authors developed a SC module for the program and

[1] Ventilation rate expressed as a factor of the space volume: ACH [-] = (ventilation induced in one hour –[m^3])/(space volume – [m^3])

performed single-day dynamic simulations, assuming three different locations for the building. Numerical investigations have also been performed to study the application of solar chimneys or similar configurations of solar heated cavities (e.g. double façades) in multi-storey buildings (Punyasompun et al. 2009, Ding et al. 2005, Letan et al. 2003, Gan 2006). The corresponding findings of these and of the parametric analysis studies are reported in the following two sections.

Parametric Analysis Findings

In parametric analysis, parameters are varied one by one to determine the sensitivity of the system's performance against each. It has been employed in the vast majority of studies and has played a substantial role in understanding the mechanisms controlling the performance of the solar chimney and their interactions. The most influential (and thus mostly studied) parameters can fall under the category of geometrical (e.g. wall height, gap width), construction (e.g. type of glass, insulation) and climatic (e.g. solar radiation, wind) parameters. Some indicative results will be presented in this section, regarding the effect of these parameters on the system's performance.

Effect of wall height and cavity width.

The effect of wall height and cavity width has in some cases been studied and expressed separately, while in others inextricably, in terms of the height-to-width aspect ratio (also referred to as height-to-gap ratio). Air flow increases with height, since the back wall's heat gains increase: in a parametric study on Trombe walls, Gan (1998) found that an increase in wall height by a quarter is equivalent to an increase in heat gains by three quarters. In the study of Ho Lee and Strand (2009) air flow rates increased in all three assumed locations of the building, by ~73% when the wall height increased from 3.5 to 9.5m (a cavity width of 0.3m was considered).

With respect to the cavity width, it was found that the induced flow rate increases with increasing width. In the analytical study of Ong and Chow (2003) it was estimated that a 0.3m wide channel induced 56% higher flow rate than one of 0.1m. Similarly, according to the model of Bassiouny and Koura (2008) a threefold increase in cavity width causes an increase of ACH by 25%. Rodrigues et al. (2000) argued that airflow rates grow with cavity width, but the growth ratios decrease as the width increases. In some studies an optimum cavity width (or optimum height-to-width ratio) was reported; for this optimum width the flow rate became maximum, while for wider gaps reverse flow occurred that reduced the mean flow through the SC (Spencer et al. 2000, Chen and Li 2001). This discrepancy between studies is attributed to the different ranges of height-to-width ratios investigated and to the influence of the inlet size. The term 'inlet' is used here to describe the opening from where the room air is admitted into the SC channel. In case the inlet size increases along with the cavity width, a lower pressure drop in the inlet can counterbalance the reduction in the flow rate caused by reverse flow, so that no optimum width is found (Gan 1998, Chen et al. 2003). Gan (2006) later reported an optimum width of 0.55m for a 6m high SC and supported that the optimum width increases with height.

Effect of inlet size.

The effect of inlet size was also explored in some studies, and was found to have a wicker effect on the performance compared to that of the cavity width. Increasing the inlet size by a factor of three increased the induced ACH by 11% in the analytical study of Bassiouny and Koura (2008), while Nouanegue and Bilgen (2009) found that volume airflow rate is a decreasing function of inlet size. Gan (1998) claimed rising airflow rates for cavity width beyond 0.3m, as long as the inlet size has the same size as the width.

Effect of inclination angle.

Various inclination angles ($15^o/30^o/45^o/60^o$) were studied experimentally by Chen et al. (2003) for a constant height, cavity width and uniform heat flux. The air velocity profile across the cavity width was found to be more uniform when the SC was inclined, leading to lower pressure losses at inlet and outlet, and thus to higher airflow rates (45% higher airflow rate was found for the angle of 45^o). Harris and Helwig (2007) numerically studied the consequences of inclining the SC along the roof line of buildings (for the latitude of Edinburgh, Scotland). They argued that although the heat gains can be favored due to tilt, heat transfer between air and glazing is higher, resulting in higher heat losses that could reduce the performance. Higher flow rates by 11% were found (for the optimum angle of 67.5^o), while the performance at 45^o angle was almost the same as that of the vertical SC. It is implicit that the impact of SC inclination is highly dependent on the latitude of the location.

Effect of back wall properties.

Increasing the thickness of the back wall (i.e its thermal mass) favors night-time ventilation because the time distribution of the induced airflow rates changes; their magnitude on the other hand is not significantly altered (Charvat et al. 2004, Martí-Herrero and Heras-Celemin 2007). Insulation of the back (and side) wall(s) is imperative to prevent devastating heat losses of the SC (as well as overheating of the adjacent spaces): airflow rates decreased by 60% without back wall insulation according to the study of Afonso and Oliveira (2000), while Gan (1998) reported that 40% of available heat gains would be lost through a non-insulated back

wall (0.3m thick). In that study the surface temperature of the back wall rose by 9°C when insulation was applied. Back wall absorptivity should be as high as possible to maximize solar heat gains. Increasing the absorptivity from 0.25 to 1, led to increased airflow rates by 42-57% in all three locations assumed for the building (Ho Lee and Strand 2009). Back wall emissivity should be as low as possible to restrict radiative heat losses; when a low-e coating was applied at the back wall, airflow rates increased by 10% in the study of Harris and Helwig (2007).

Effect of glazing type.

The use of double glazing can prevent downdraught (and thus reverse flow) along the cold glass surface during winter, but was also found to increase the induced airflow rates up to 17% when applied to a Trombe wall used for passive ventilation in the summer (Gan, 1998). Harris and Helwig (2007) argued that double glazing improves the performance of a SC but only marginally, so that it is not a cost-effective measure (only summer conditions were considered).

Effect of climate: solar intensity and wind.

The intensity of solar heat flux is the motive force for the operation of the SC and is thus the most determinant factor for its performance. In the experimental study of Chen et al. (2003) varying values were considered for the uniform heat flux on the back wall and the airflow rate was found to rise by ~38% for a threefold increase of heat flux (from 200W/m^2 to 600W/m^2). Mathur et al. (2006) found that airflow rate increases linearly with solar radiation and Bansal (1993) estimated that a SC with surface area of 2.25m^2, would induce 100m^3/hr and 350m^3/hr for solar radiation of 100W/m^2 and 1000W/m^2 respectively. Based on experimental investigations on a small-scale SC, Burek and Habeb (2007) derived that the mass flow rate is proportional to $Q_i^{0.572}$ where Q_i (W/m^2) the uniform heat flux supplied to the back wall. The simulations of Ho Lee and Strand (2009) showed flow rates to vary as much as 200% between the three assumed locations of the building, as a result of the varying solar availability.

Wind is the second most influential climatic parameter, as it can create positive or negative pressures at the outlet of the SC and thus obstruct or enhance the airflow. In the outdoor experiments by Arce (2009) at a full-scale SC, the highest airflow rates coincided with the highest recorded wind velocity, while Afonso and Oliveira (2000) altered their model to include wind effects which proved significant (error between model predictions and measurements was then lower than 10%). In the analytical study of Mathur et al. (2006) the large error of 23% was attributed to wind effects, which were neglected in the model. In practice, devices can be incorporated at the outlet of the SC so that wind of all directions creates negative pressures.

Integration in Multi-Storey Buildings

Investigating the performance of a SC in a multi-storey building holds great interest due to the high potential benefits involved in actual, large-scale applications. This subject has been studied only numerically in the past few years, mainly with CFD simulations assuming steady-state temperature and air velocity fields. The CFD models were validated against small-scale experimental data.

Passive ventilation of a five-storey building was found feasible in the study by Letan et al. (2003). Numerical simulations were performed with commercial CFD software assuming steady-state temperature and velocity fields and summer conditions. It was found that the induced airflow rates decreased with floor height: the lower the floor, the higher the airflow rate. Acceptable thermal conditions were found for the first four floors with air temperatures close to that of the incoming air (at maximum 25.5°C), while the fifth floor was overheated up to 29.9°C. The authors argued that extending the SC by one storey height would improve the situation, but mechanical ventilation would still be required for the top floor.

Ding et al. (2005) investigated a prototype eight-storey office building with an atrium on the northern side and a double-skin façade on the southern side, which extends to a SC channel above the roof height. Reduced scale experiments and CFD simulations were employed in this study. The size of the openings connecting the atrium to the occupant spaces were fixed, while for the size of the openings between the floor spaces and the double-skin channel three values were tested (1m^2/2m^2/4m^2 per floor). Different heights for the SC were also examined. Here as well the airflow rates got lower with floor level. By increasing the openings' size higher airflow rates resulted at all floors, but the pressure difference at the upper floors got lower, resulting in lower percentage of the overall flow going through these. The authors recommended that the SC should be at least two-storey high.

Ventilation of a four-storey building (total height of 12m) via buoyancy-induced flow in a double-skin façade channel was studied by Gan (2006) using CFD analysis. Although not a SC channel was studied here, the double-skin façade works in a similar way, with the difference of more symmetrical heating of the two glass skins. Varying cavity widths for the double-façade channel and different exhaust configurations from the floors to the channel were investigated. Replacing the outer skin of the façade with photovoltaic panels (PV) was also examined. For the design where each floor has its own opening

to the double-skin channel (referred to as 'room ventilation' in the study), flow rates decreased from bottom to top, due to lower stack heights in the upper levels: for a cavity width of 0.4m, 34% and 17% of the total flow was induced at the bottom and top floor respectively. These floor-to-floor variations were significantly reduced when PV panels were integrated at the outer skin of the façade. For this four-storey structure a cavity width of 0.6-0.8 is proposed as optimum for the 'room ventilation' design.

Punyasompun et al. (2009) performed small scale experiments for a three-storey building under the Bangkok climatic conditions and developed a simplified model that could be used for designing a 'multi-solar chimney building'. They tested two possible ways of SC integration; one where each floor had a separate SC channel (i.e. outlet openings at every floor), and one where the floors were connected to a common SC channel, extending from bottom to top floor (i.e. one outlet opening at the top of the channel). The latter proved to perform better and induce higher airflow rates in the floors.

Concluding Remarks

It is evident that fair background knowledge has been gained so far on the physical mechanisms and the various parameters affecting the performance of SC systems. The potential of SC systems to drive airflow and achieve sufficient passive ventilation in buildings has been explored in several studies and was found satisfactory. Most of these studies however, involved single-room or single-zone buildings and assumed steady-state conditions, while most of the outdoor experimental studies (subjected to dynamic climatic conditions) were performed for hot and arid climates and specific building types, typical of the location. Recent studies have demonstrated the additional complexity and challenges posed by integrating a SC system with a multi-storey building, indicating the need for further research on various related topics.

In practice and for large-scale applications of SC systems in buildings, it is imperative that the design be based on performance estimations for dynamic conditions and for the specific building, climate and surroundings. Numerical modeling in building performance simulation (BPS) tools should be employed when it comes to practical applications: dynamic thermal and airflow simulations for the SC-building system can be performed and the feasibility, potential benefits as well as possible improvements of the design can be fully explored.

This project studies the feasibility of a SC integrated in a prototype multi-storey office building in the Netherlands. Performance simulations will be performed in the BPS tool ESP-r and results will be used for sensitivity analysis (SA) and Optimization of the design. At present only the SA results are available. The calibration procedure and the SA results are presented in the following sections.

AIM

The aim of this part of the project is the investigation of the applicability and optimization of a solar chimney to enhance natural ventilation in a multi-storey office building in the Netherlands.

METHODOLOGY

To achieve the aim of the project we envisaged the research methodology which involves the following stages (Fig. 3):

1. Calibrating the model of the solar chimney with the available data from the small-scale measurements set-up.
2. Performing Sensitivity Analysis (SA) for a SC design and for the following parameters: length, cavity width, inside face short-wave absorptivity and long-wave emissivity, insulation thickness and thermal mass of the back and side walls, glazing type and glass percentage of the glazed wall. For the selected range of variance of the aforementioned parameters, the Latin Hypercube sampling method is employed and 200 samples

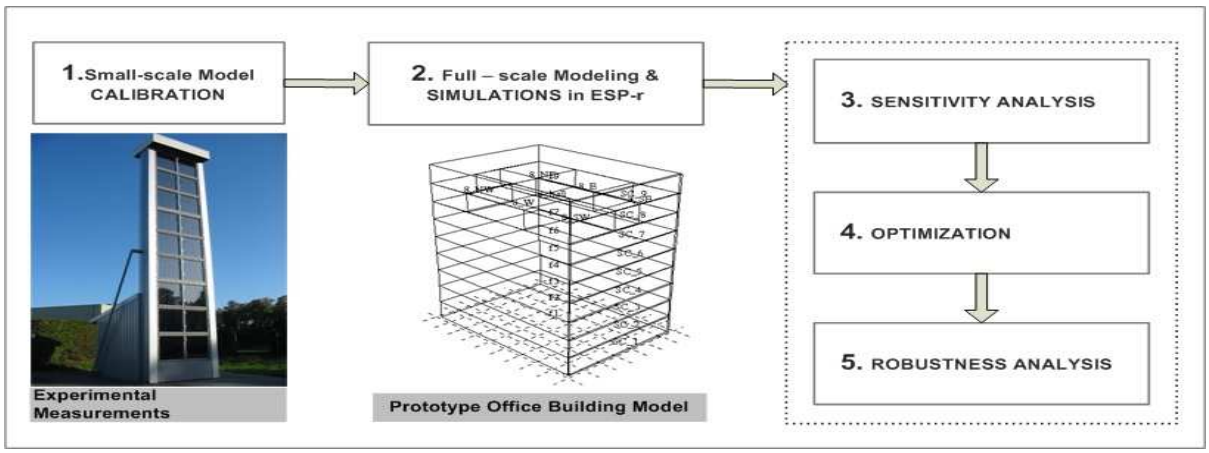

Figure 3. Applied Methodology.

are generated in total. These are translated to an equal number of sets of input files for ESP-r and SA is based on the produced sets of simulation results. The performance indicators for the SA are (i) the annual harvested energy (i.e. the air enthalpic gains in the SC) and (ii) the annual fan energy savings.

3. Multi-objective optimization of the SC design to maximize: (i) the air enthalpic gains in the SC that could be recovered and used for e.g. heating purposes and (ii) the fan energy savings.
4. Testing the robustness of the final optimized design using the model of the SC integrated to the model of the prototype building (e.g. influence of operating windows, alternate design for air supply etc).

At the absence of results for stages [4 & 5], the calibration and SA results are reported in the next sections. A short description of the case study building is also included in the last section.

CALIBRATION

Calibration Procedure

The objective of the procedure is to calibrate the airflow components of the SC model so that pressure losses, airflow rate and temperatures in the SC channel are predicted reliably. The calibration is based on available data from experimental measurements performed in a small-scale SC test set-up, constructed in the context of the 'Earth, Wind & Fire' project and located in Mook, Netherlands. Calibration was performed of the ESP-r model of the test set-up (i.e. a small-scale SC), which was created in line with the physical model in terms of geometry and materials. A presentation of the test set-up and calibration methodology follows.

The small-scale test set-up.

The SC test set-up (Fig. 4[a]) is 11m high, the channel is 2m long and 0.25m wide (width-to-height ratio is 1:44). An aluminum layer with absorptivity of 0.95, emissivity of 0.05 and thickness of 0.5mm is used for the inside surfaces of the back and side walls. The walls are well insulated to the outside (U-value = 0.16 W/m^{2}K) and a double glazing (U-value = 1.32 W/m2K) is used with a visible light transmission factor of 0.56 and low-e coating on both glass panes. The SC channel is connected at its bottom to a small room (volume is ~20m^3) intended to pre-condition the incoming air up to 20^{o}C. Air flows naturally into the room through a window located at its north side (opening is ~1m^2) and into the solar chimney channel through an inlet opening located close to the floor level (at 0.25m) and which has the same area and shape as the cross section of the SC.

An extensive measurements' schedule was designed but will not be presented here for brevity reasons. The data used for the calibration include: (i) inside surface temperatures for the glazing, back and side walls at single points and four heights along the SC channel (0.5/4.0/7.5/9.5m), (ii) air temperatures at nine points evenly distributed over the channel's cross-section and at four heights (0.25/4.0/7.5/11m), (iii) pressure difference between inlet and outlet of the channel and (iv) air velocities at two single points of the cross-section at four heights (0.25/4.0/7.5/11m). Due to unfavorable weather conditions and costs involved, measurements were performed for a limited number of days from December till April. Measurements from 15/12/09, 08/01/10 and 15/04/10 were used for calibration.

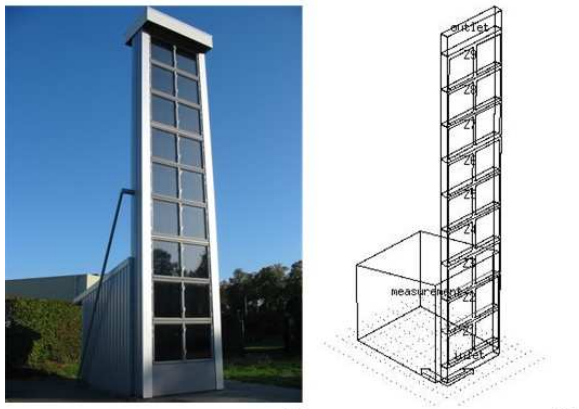

Figure 4[a,b]. The small –scale experimental set-up (a) and its model counterpart in ESP-r (b).

Calibration in ESP-r.

The airflow through the SC is modeled using the 'general flow conduit' component, which is assumed the equivalent of a duct. The required input parameters for this component are the hydraulic diameter [m] (equal to the diameter in case of a round duct), cross-section surface area [m^2], length [m], roughness [m] and local dynamic loss factor [-]. From the above parameters the first three are fixed as they are determined by the geometry of the SC duct, while the roughness and local loss factor are the parameters to be calibrated.

Due to restrictions in the ESP-r program, it was not possible to impose transient measured boundary conditions; instead measurement data corresponding to one-hour timeslots were used and calibration was performed assuming steady-state conditions for these hours. Surface temperatures and pressure difference along the channel are the boundary conditions (input) to the model. The output data (air temperatures and mass flow rate) are compared to the corresponding measured values and the model is calibrated until reasonable agreement is accomplished. For the air temperature measurements, the statistical measure of

R-squared (R^2) is used to judge statistical correlation which can take values from 0 to 1, with 1 being the absolute agreement between measurements and model predictions. Since the SC is modeled in ESP-r with nine thermal zones over the height (see Fig. 4[b]), i.e. model's input and output data refer to nine points representing the average conditions in the zones, the available measured data (at four heights) were fitted linearly with curves and 'measured' values were estimated for the nine model heights, so that the calculation of the R^2 is possible. The R^2 value of the linear fitting curves was usually above 0.90, indicating a linear relationship between height and air temperature in the SC.

It is noted that the measured mass flow value, derived from velocity measurements at two points of the SC cross-section (at four different heights), is assigned an error of 40%, which is the maximum variation between points along the length and width of the SC channel, found in measurements performed specifically to have an idea of the velocity profile distribution in the channel. Therefore, a valid range of ±40% around the measured mass flow value is estimated, within which the predicted value should fall.

Calibration Results & Discussion

The calibration procedure outlined in the previous section was performed for ten timeslots. It is noted that the roughness parameter was found to have negligible effect in the predictions, therefore it was fixed at 1mm and calibration consisted of adjusting the local loss factors of the SC components (Ci). In all cases a loss factor value between 0.6 and 1.0 was found to be appropriate (for each timeslot a different value gave the best results) but since this value is a fixed input parameter in the model, results are presented here for a Ci value of 1.0. Agreement between model predictions and measurements with respect to air temperatures for every timeslot is presented in Table 1, expressed with the value of R^2, while agreement of measured and predicted mass flow rates is presented in Table 2, where predicted values should fall with the valid range. For brevity reasons in Table 2 only the number of the timeslot is included; for more data one can refer to Table 1.

Given the errors introduced by pre-processing of the measured data (e.g. data fitting with curves and assumption for the surface temperatures of the walls at the upper part of the SC) the model's performance is considered satisfactory and the calibration procedure successful. In most cases the R^2 value is above 0.70, whereas lower values are found at times of low solar radiation intensity values (e.g. timeslot no.5) or for the timeslots of 15/4/10, where a significant error is traced back to the trendline of the surface temperatures. Wind speed is also high during this day, which could account for the poor performance of the predictions, since wind is neglected in the model.

The above are an indication that the model (where the C_i value is fixed) will not be able to represent mass flow and air temperatures accurately in some hours of the day where extreme conditions, in terms of solar radiation and/or wind speed might come to play a role in the real system. The complexity of flow characteristics in a naturally ventilated duct and the various parameters that affect the flow cannot possibly be all represented equally well in a model, which is a simplification of the real system.

The calibrated model was also validated for whole-day dynamic conditions and results were found to be satisfactory. Validation results are not presented here for brevity reasons. Confidence acquired in the ESP-r model of the SC through validation allows us to use it for the simulation predictions required in the next steps.

Table 1. Calibration results: air temperature agreement between measurements and model predictions

			Loss Factor	
	Date	**Timeslot**	**Ci [-]**	**R^2 [-]**
1	15/12/09	10:00-11:00	1.0	**0.95**
2	15/12/09	12:00-13:00	1.0	**0.71**
3	15/12/09	13:00-14:00	1.0	**0.97**
4	15/12/09	14:00-15:00	1.0	**0.90**
5	15/12/09	15:00-16:00	1.0	**0.27**
6	08/01/10	11:00-12:00	1.0	**0.81**
7	15/04/10	12:00-13:00	1.0	**0.30**
8	15/04/10	13:00-14:00	1.0	**0.80**
9	15/04/10	14:00-15:00	1.0	**0.41**
10	18/03/10	12:00-13:00	1.0	**0.95**

Table 2. Calibration results: mass flow rate agreement between measurements and model predictions.

	Predicted	**Measured**	**Valid range**
	m_{pred} [kg/s]	**m_{meas} [kg/s]**	**$0.6m_{meas}$ - $1.4m_{meas}$**
1	**0.76**	0.55	**0.33 - 0.77**
2	**0.77**	0.54	**0.32 - 0.76**
3	**0.76**	0.63	**0.38 - 0.88**
4	**0.73**	0.58	**0.35 - 0.81**
5	**0.69**	0.62	**0.37 - 0.87**
6	**0.68**	0.73	**0.44 - 1.02**
7	**0.52**	0.60	**0.36 - 0.84**
8	**0.54**	0.57	**0.34 - 0.80**
9	**0.53**	0.59	**0.35 - 0.83**
10	**0.60**	0.58	**0.35 - 0.81**

CASE STUDY

Some information regarding the prototype building is presented here, since the sensitivity analysis is performed for a SC design intended to work for the specific building. The case study is

based on a simplified model of the faculty of Architecture at the Eindhoven University of Technology (TU/e) campus, in the Netherlands. The floor plan of the building is rectangular with dimensions of 43.2*32.4m (floor surface area is ~1400m^2). The 32.4m dimension, corresponding to the southern and northern façade determines the maximum possible length of the SC (see next section). The total building height is 49.5m (9 floors of 5.5m height each), and ventilation requirements are estimated at 32.66 m^3/s (3.63m^3/s for each floor). Outdoor air enters the building through a main supply duct on the northern side (conditioning of the air is assumed up to 18^{o}C in the supply duct), diverges into the floors and is consecutively exhausted in the main exhaust duct on the southern side (exhaust air temperature is 20^{o}C). The SC channel is connected to the exhaust duct at ground level; a fan located at the bottom of the SC will guarantee an airflow of 32.66 m^3/s at all times. The pressure drop through the duct network of the building (excluding the SC channel) was estimated to be aprox. 40Pa. Dampers are located at each floor level to balance the system and ensure that all floors receive the same airflow rate. The building is assumed to be an office building, thus the functional hours are from Monday to Friday and from 7am to 7pm (3132 hours per year).

SENSITIVITY ANALYSIS

Sensitivity analysis is performed for a full-scale SC of 50m height, intended to be integrated with the prototype office building previously described. The parameters considered in the SA are presented in Table 3, along with the corresponding ranges and step changes; discrete values and uniform distributions were considered for each parameter.

Table 3. Parameters and their range of values considered for SA.

		Range of Values			
	Parameter	**Lower**	**Upper**	**Step**	**Unit**
1	Length	7.2	32.4	1.8	[m]
2	Cavity width	0.7	2	0.1	[m]
3	Thermal mass	0.001	0.1	0.005	[m]
4	Insulation	0.001	0.12	<0.02	[m]
5	Absorptivity	0.05	0.95	0.2	[-]
6	Emissivity	0.05	0.95	0.2	[-]
7	Glazing type	Single, Double, Low-e		-	-
8	Glass percentage	0.7	0.95	0.05	[-]

With the term ‘thermal mass’ the thickness of a concrete layer placed behind the absorbant layer[2] of the back and side walls is considered. Absorptivity (short-wave) and emissivity (long-wave) are material properties of the absorbant layer. Three glazing types are taken into account (single, double and low-e) with a visible light transmission value of 0.87, 0.76 and 0.79 respectively. Restrictions were imposed so that the cavity width is less than 25% of the length (to avoid shading) and that the cross-section area of the SC results in air velocities not more than 3m/s in the SC shaft. The parameter ‘glass percentage’ is considered to account for the reduction of the total glazed area due structural framing of the glazing wall. The parameters (independent variables) were sampled simultaneously using the Latin Hypercube Sampling method and 200 samples were generated (for the matrix generation the freeware tool Simlab was used). The performance indicators considered for the SA (dependent variables) are (i) the annual harvested energy in KWh and (ii) the annual fan energy savings in KWh.

The annual harvested energy is calculated as the sum of the air enthalpic gains in the SC for all functional hours:

$$E_{harvest=}\sum(\dot{V} * \rho_{in} * c_p * (T_{out} - T_{in})\ [KWh] \quad (1)$$

Where $\dot{V}$ [m^3/s] the volume flow rate through the SC, ρ_{in} [kg/m^3] the air density of the incoming air, c_p [KJ/kgK^{-1}] the specific heat capacity of air at the inlet temperature, T_{out} [^{o}C] the air temperature at the outlet of the SC and T_{in} the temperature of the incoming air, assumed to be 20^{o}C.

The annual fan energy savings are calculated as the sum for all functional hours of the quantity:

$$E_{fan} = \sum \frac{\Delta P_{sc} * \dot{V}}{\eta}\ [Wh] \quad (2)$$

With $\dot{V}$ the building volume flow rate equal to 32.66 m^3/s, η=0.65 [-] the fan’s efficiency and ΔP_{sc} the pressure difference induced by the SC equal to:

$$\Delta P_{sc} = (\rho_{supply} - \rho_{sc}) * g * H - \Delta P_{loss,sc}\ [Pa] \quad (3)$$

with ρ_{supply} [kg/m^3] the density of the air at the supply duct (temperature of supply air is assumed 18^{o}C), ρ_{sc} [kg/m^3] the air density at the SC channel and $\Delta P_{loss,sc}$ [Pa] the pressure losses (local dynamic and friction losses) of the SC. In case ΔP_{sc} results a negative quantity the energy savings are set to zero for that hour, since a negative value would mean that the fan would have to consume more power to account for the SC’s high losses. It is reminded that the fan would need to generate a pressure difference ΔP_{fan} equal to:

$$\Delta P_{fan} = \Delta P_{build} - \Delta P_{sc} = 40 - \Delta P_{sc}\ [Pa] \quad (4)$$

[2] the term is used here for the surface material of the opaque walls of the SC, which is usually a low thermal mass layer with a dark-coloured outer surface for maximum solar radiation absorption.

For the total of 200 samples, simulations were performed in ESP-r and the two performance indicators were derived for each sample. The method of standardized regression coefficients (SRC) was used to analyze the results, which is a linear regression method. For every performance indicator (harvested energy and fan savings) the parameters of the SA are assigned an SRC value between 0 and 1, which indicate the sensitivity of the model output to that parameter. The higher the SRC value, the more sensitive the model (i.e. the performance indicator) to that parameter. A positive value of the SRC means that a positive change of the parameter's value will result in a positive change of the performance indicator. A negative SRC value means that for a positive change of the parameter a negative change of the performance indicator is expected. Results of the SA are presented in the next section.

SA Results

For each performance indicator, the ranking of the eight parameters, starting from the most influential, and the SRC values are presented in Table 4. It is noted that the R-square values are 0.875 for the harvested energy model and 0.871 for the fan energy savings model, reassuring that the linear regression method was a good choice; in case these values were low a non-linear regression analysis would have been more appropriate.

Table 4. Ranking of the SA parameters.

rank	Harvested energy	SRC	Fan energy savings	SRC
1	length	0.747	length	0.817
2	absorptivity	0.538	gap width	0.556
3	glazing type	0.237	glazing type	0.116
4	thermal mass	-0.231	thermal mass	-0.113
5	glass percentage	0.175	absorptivity	0.089
6	insulation thickness	0.066	glass percentage	0.081
7	gap width	0.025	insulation thickness	-0.023
8	emissivity	0.000	emissivity	0.023

For the harvested energy the most important parameters are the length of the SC, the short-wave absorptivity of the walls, the glazing type (the positive SRC value here means a double is preferable to a single glazing and that the low-e would be the best choice out of the three) and the thermal mass. For the fan energy savings only the second most influential parameter is different compared to harvested energy, and that is the gap width, which ranks only 7th in the harvested energy model. Parameters 5 to 6 are not as important, whereas the ones ranking 7th and 8th could be discarded from the regression model (the p-value is more than 0.05)[3]. It should be noted that the ranking of the insulation thickness is low because the backwall of the SC is assumed to be in contact with the wall of the exhaust duct, where the air temperature is 20°C. The negative value of the SRC for the thermal mass indicates that it is preferable to have the lower thermal mass possible in the walls construction in order to maximize harvested energy and fan energy savings.

From the results of the 200 simulations a scatter-plot is produced with the x-axis being the harvested energy and the y-axis the fan energy savings; each dot corresponds to one sample. It can be derived from Figure 5 that the two performance indicators are not conflicting, i.e. there will be a solution that will maximise both, as is for example the solution encircled in the figure. It can also be seen that a large number of solutions results in zero fan energy savings (or increased required fan power).

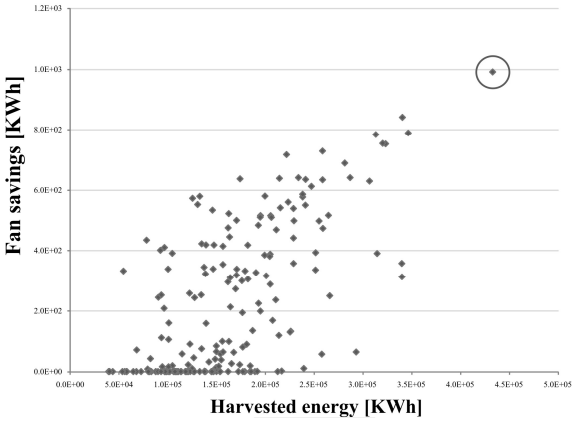

Figure 5. Scatter-plot of the 200 simulation results.

CONCLUSIONS

The applicability of a SC for passive ventilation of a prototype multi-storey office building in the Netherlands is explored. Measurement data in a small-scale SC were used to calibrate and validate the SC model. Modeling and simulations were performed in the building simulation tool ESP-r. A case study office building has been chosen and a sensitivity analysis (SA) of a SC design intended for this building was performed. The dimensions of the SC (length and gap width), the short-wave absorptivity of the walls, the glazing type and thermal mass were identified as the most influential parameters with respect to the annual harvested energy in the SC and the annual fan energy savings. The next step is the optimization of the SC design and at the final stage a robustness analysis of the optimized design against -among others- active user behavior (e.g. opening of windows). At the final stage the integrated model of the SC and the office building will be used.

[3] The p-value is the probability that the true SRC is zero. If p-value is higher than 0.05 the variable should be discarded from the model.

REFERENCES

Afonso, A. and Oliveira, A. 2000. Solar chimneys: simulation and experiment. Energy and Buildings 32: 71-79.

Arce, J., Jimenez, M.J., Guzman, J.D., Heras, M.R., Alvarez, G., Xaman, J. 2009. Experimental study for natural ventilation on a solar chimney. Renewable Energy 34:2928-2934.

Awbi, H.B. and Gan, G. 1992. Simulation of solar-induced ventilation. Renewable Energy Technology and the Environment 4:2016-30.

Bansal, N.K., Mathur, R., Bhandari, M.S. 1994. Solar chimney for enhanced stack ventilation. Building and Environment 28:373-377.

Barozzi, G.S., Imbabi, M.S.E., Nobile, E., Sousa, A.C.M. 1992. Physical and numerical modeling of a solar chimney-based ventilation system for buildings. Building and Environment 27:433-445.

Bassiouny, R. and Koura, N.S.A. 2008. An analytical and numerical study of solar chimney use for room natural ventilation. Energy and Buildings 40:865-873.

Borgers, T.R. and Akbari, H. 1979. Laminar flow within the Trombe wall channel. Solar Energy 22:165-174.

Bouchair, A. 1994. Solar chimney for promoting cooling ventilation in southern Algeria. Building Services Engineering Research and Technology 15(2):81-93.

Burek, S.A.M. and Habeb, A. 2007. Air flow and thermal efficiency characteristics in solar chimneys and Trombe walls. Energy and Buildings 39:128-135.

Charvat, P., Jicah, M., Stetina, J. 2004. Solar chimneys for ventilation and passive cooling. World Renewable Energy Congress, Denver, USA.

Chen, Z.D., Bandopadhayay, P., Halldorsson, J., Byrjalsen, C., Heiselberg, P., Li, Y. 2003. An experimental investigation of a solar chimney model with uniform wall heat flux. Building and Environment 38:893-906.

Chen, Z.D. and Li, Y. 2001. A numerical study of a solar chimney with uniform wall heat flux. In: Proceedings of the Fourth International Conference on Indoor Air Quality, Ventilation and Energy Conservation in Buildings, Human, China, p.1447-54.

Ding, W., Hasemi, Y., Yamada, T. 2005. Natural ventilation performance of a double-skin façade with a solar chimney. Energy and Buildings 37:411-418.

Gan, G. and Riffat, S.B. 1998. A numerical study of solar chimney for natural ventilation of buildings with heat recovery. Applied Thermal Engineering 18: 1171 -1187.

Gan, G. 1998. A parametric study of Trombe walls for passive cooling of buildings. Energy and Buildings 18:1171-87.

Gan, G. 2006. Simulation of buoyancy-induced flow in open cavities for natural ventilation. Energy and Buildings 38:410-420.

Gan, G. 2010. Impact of computational domain on the prediction of buoyancy-driven ventilation cooling. Building and Environment 45:1173-1183.

Harris, D.J., Helwig, N. 2007. Solar chimney and building ventilation. Applied Energy 84:135-146.

Hirunlabh, J., Kongduang, W., Namprakai, P., Khedari, J. 1999. Study of natural ventilation of houses by a metallic solar wall under tropical climate. Renewable Energy 18:109-119.

Ho Lee, K. and Strand, R.K. 2009. Enhancement of natural ventilation in buildings using a thermal chimney. Energy and Buildings 41:615-621.

Khedari, J., Boonsri, B., Hirunlabh, J. 2000. Ventilation impact of a solar chimney on indoor temperature fluctuation and air change in a school building. Energy and Buildings 32:89-93.

Khedari, J., Rachapradit, N., Hirunlabh, J. 2003. Field study of performance of solar chimney with air-conditioned building. Energy 28:1099-1114.

Martí-Herrero, J., Heras-Celemin, M.R. 2007. Dynamic physical model for a solar chimney. Solar Energy 81:614-622.

Mathur, J., Bansal, N.K., Mathur, N.K., Jain, M., Anupma. 2006. Experimental investigations on solar chimney for room ventilation. Solar Energy 80:927-935.

Nouanégué, H.F. and Bilgen, E. 2009. Heat transfer by convection, conduction and radiation in solar chimney systems for ventilation of dwellings. International Journal of Heat and Fluid Flow 30:150-157.

Ong, K.S. and Chow, C.C. 2003. Performance of a solar chimney. Solar Energy 74:1-17.

Punyasompun, S., Hirunlabh, J., Khedari, J. Zeghmati, B. 2009. Investigation on the application of solar chimney for multi-storey buildings. Renewable Energy 34:2545-2561.

Rodrigues, A.M., Canha da Piedade, A., Lahellec, A., Grandpeix, J.Y. 2000. Modeling natural convection in a heated vertical channel for room ventilation, Building and Environment 35:455-469.

SIMLAB. 2009. Version 3.2 Simulation Environment for Uncertainty and Sensitivity Analysis, developed by the Joint Research Centre of the European Commission.

Spencer, S., Chen, Z.D., Li, Y., Haghighat, F. 2000. Experimental investigation of a solar chimney natural ventilation system. In: Proceedings of Room Vent, Seventh International Conference on Air Distribution in Rooms, Reading, UK, 9-12 July, p.813-8.